Applied Geochemistry 100 (2019) 121–130

Contents lists available at ScienceDirect

Applied Geochemistry

journal homepage: www.elsevier.com/locate/apgeochem

Effects of γ-alumina nanoparticles on strontium sorption in smectite: Additive model approach

Natalia Mayordomo[1], Ursula Alonso[*], Tiziana Missana

CIEMAT, Department of Environment, Avda. Complutense 40, 28040, Madrid, Spain

ARTICLE INFO

Keywords:
Strontium
Smectite
Alumina
Nanoparticles
Sorption modelling
Additive model

ABSTRACT

Strontium sorption was analysed in binary mixtures of smectite and γ-alumina nanoparticles under different pH, ionic strength and Sr concentration. The aims were to verify if γ-alumina nanoparticles enhance Sr sorption in smectite and to analyse whether a component additive model satisfactorily described Sr sorption in the mixtures.

In smectite, Sr sorption mainly occurs by cation exchange but surface complexation was also accounted for. In both solids, surface complexation was described with a non-electrostatic model.

The addition of γ-Al_2O_3 nanoparticles to smectite improved Sr uptake under alkaline pH and high ionic strength, and the additive model successfully reproduced experimental data. In contrast, under acid pH and low ionic strength, no sorption improvement was observed upon adding the nanoparticles and the additive model overestimated Sr sorption. The competition of Al^{3+} ions, coming from γ-Al_2O_3 dissolution, partially explained the differences between data and model. Nevertheless, surface interactions between alumina particles and smectite layers may be shielding the charge, hindering contaminant access to exchangeable sites in smectite.

1. Introduction

Strontium is an alkaline earth metal characterised by relatively simple chemistry, being +2 the only stable oxidation state. Strontium presence is natural and anthropogenic, from milling processes, coal burning, fertilizers (WHO, 2010) and from nuclear industry. The radioactive strontium isotope ^{90}Sr is a fission product with a half-life of 28.8 years. Its release in the environment is of great concern during the explosion of nuclear weapons or after nuclear accidents like Chernobyl (IAEA, 2006) or Fukushima (Rosenberg et al., 2017; Sahoo et al., 2016). In the body, Sr can replace Ca^{2+} in the bones or can inhibit vitamin production and it is related to leukaemia, rickets and renal diseases (Nielsen, 2004).

For the remediation of Sr contaminated sites, different materials and methods have been proposed, to favour precipitation, membrane immobilization and ion exchange mechanisms (MacMillan et al., 2000). The effectiveness of Sr sorption depends on the material properties and on the chemical conditions (Li et al., 2016; Metwally et al., 2017).

Several Sr sorption studies onto soils and sediments are available (Fuller et al., 2016; McKinley et al., 2007; Smiciklas et al., 2015a, 2015b) and, in particular, in the materials used as barriers in geological repositories for nuclear waste (Pusch et al., 2015), like sedimentary rocks or smectite clay (Galamboš et al., 2010; Jeong et al., 1996; Kasar et al., 2017; Missana and Garcia-Gutierrez, 2007; Missana et al., 2008; Ohnuki and Kozai, 1994; Pathak, 2017; Rafferty et al., 1981; Savoye et al., 2015; Siroux et al., 2017; Testoni et al., 2017; Yu et al., 2015). Additionally, Sr retention on different pure nanomaterials (Ahmadi et al., 2015; Kayvani Fard et al., 2017; Metwally et al., 2017; Mukhopadhyay et al., 2015; Ryu et al., 2016) and on metal oxides has been also analysed: in silica (Zhang et al., 2015), titanium oxide (Voronina and Semenishchev, 2016), iron oxide (Mukhopadhyay et al., 2015; Tu et al., 2015) or aluminium oxides (Asztemborska et al., 2016; Bonner et al., 1966; Sid Kalal et al., 2016) and hydroxides (Katz et al., 2013; Kinninburgh et al., 1975).

However, few sorption studies for mixed solids are reported: bentonite and granite (Lee et al., 1997), clays and sand (Yu et al., 2015), smectite and illite (Missana et al., 2008) or montmorillonite and zeolite (Basçetin and Atun, 2010).

In general, to predict the retention of contaminants in complex environments, consisting of mixtures of different clays, minerals and oxides, it is not an easy task. The empirical procedure can be used, and retention can be directly measured but, this method is not predictive beyond the specific conditions of the measurements (Smith, 1999). Thermodynamically-based sorption models (SMs) can be also applied (Dzombak and Morel, 1990; Davis et al., 1998). These models define the solid surface as a set of reactive functional sites, which form

* Corresponding author.
E-mail address: ursula.alonso@ciemat.es (U. Alonso).
[1] Present address: Helmholtz-Zentrum Dresden-Rossendorf (HZDR), Institute of Resource Ecology, Bautzner Landstraβe 400, 01328 Dresden, Germany.

https://doi.org/10.1016/j.apgeochem.2018.11.012
Received 27 February 2018; Received in revised form 15 November 2018; Accepted 17 November 2018
Available online 19 November 2018
0883-2927/

different types of complexes with dissolved solutes. The difficulties arise when applying SMs to describe the retention behaviour of contaminants onto complex mineral assemblages (Anderson and Benjamin, 1990). Then, two approaches can be used: to analyse the mixture of solids as a whole, or to use the component additive approach (Davis et al., 1998). The problem of the first approach is that defining the surface properties of a mixture of solids (like for example its surface area or their site densities) is not straightforward. The component additive approach has the advantage of making use of previous knowledge and of available SMs, developed for the pure solids, but additivity is not always verified and seems to be system-dependent (Davis et al., 1998; Landry et al., 2009; Comarmond et al., 2012; Honeyman and Santschi, 1991). The sorption of a system is expected to be additive when the components do not interact or when their interactions do not affect their surface properties, diminishing contaminant retention in the mixtures (i.e. Alessi and Fein, 2010).

Smectites are used as barriers for nuclear waste disposal (Pusch et al., 2015), amongst other reasons, because they exhibit a permanent negative charge, giving high capacity to absorb cations, mainly by cation exchange mechanism. Smectite ability to retain anionic species is limited to the availability of positively charged surface sites at layer edges.

In a recent study, the addition of γ-Al_2O_3 nanoparticles to smectite was proposed to improve the retention capacities for anionic species, in particular of selenite (Mayordomo et al., 2016). The high sorption capacities of aluminum oxides (Hua et al., 2012; Karamalidis and Dzombak, 2010; Kasprzyk-Hordern, 2004; Shirai et al., 2009) and their increased surface area, in nanoparticulate state, made them good candidates to promote the retention of contaminants (Khin et al., 2012; Kuiken, 2010; Sharma et al., 2009). Complementary stability studies (Mayordomo, 2017) revealed that, under acidic conditions, when smectite and γ-Al_2O_3 nanoparticles were mixed, particle (hetero)aggregation was fast promoted, what may compromise retention properties. In the case of selenite (Mayordomo et al., 2016), whose main aqueous species are anionic, sorption takes place by surface complexation mechanisms in both smectite and alumina and sorption in smectite/alumina mixtures could be perfectly described by the additive model approach. Nothing suggested that particle interactions in the mixture had an effect on selenite sorption (Mayordomo et al., 2016).

The aims of this study are to analyse whether Sr sorption on smectite is improved by the addition of γ-Al_2O_3 nanoparticles and to verify whether Sr sorption on smectite/γ-Al_2O_3 (S/A) mixtures can be described with the SMs developed for the pure solids.

To analyse the case of Sr is particularly interesting, because Sr sorption in smectite is independent of pH, decreases as the ionic strength increases, and mainly occurs by cation exchange mechanism (Basçetin and Atun, 2010; Missana and Garcia-Gutierrez, 2007; Missana et al., 2008; Pathak, 2017; Siroux et al., 2017; Smiciklas et al., 2015a, 2015b). Only under high alkaline pH, Sr^{2+} surface complexation at the clay edge sites is considered (Kohlicková and Jedináková-Kcižová, 1998; Missana and Garcia-Gutierrez, 2007; Missana et al., 2008; Ohnuki and Kozai, 1994; Yu et al., 2015) and its contribution is less relevant for Sr than for other divalent metal cations, like cobalt (Missana and Garcia-Gutierrez, 2007) or zinc (Baeyens and Bradbury, 1997; Bradbury and Baeyens, 1997).

To achieve our goals, Sr sorption was first analysed on the pure systems. Previous studies on Sr sorption on smectite were considered. The model used to describe Sr sorption, which included cation exchange and one-site non-electrostatic surface complexation of Sr^{2+} (Missana and Garcia-Gutierrez, 2007; Missana et al., 2008) was used as a starting point.

Sr retention on γ-Al_2O_3 and on S/A mixtures was analysed under a wide range of pH, ionic strengths, Sr concentrations and S/A mixture compositions. The chemistry of water at equilibrium was incorporated to the SMs and relevant aspects that may affect sorption properties in the mixtures, like competition of ions coming from solid dissolution, were experimentally and theoretically analysed to roundly verify the applicability of a sorption model based on component additive approach.

2. Materials and methods

2.1. Materials

Smectite was obtained from FEBEX bentonite (Almería, Spain), a Ca−Mg smectite with high smectite content (Huertas et al., 2000). For sorption experiments, the clay was purified and sodium homoionised (Na-smectite), by washing it three times with 1 M $NaClO_4$. To extract the colloidal fraction (particles < 1 μm), the samples were centrifuged several times at 600 g for 10 min and the supernatant was collected. Suspensions were equilibrated by dialysis (using 7 Spectra/Por membranes MWCO 3500) with $NaClO_4$ electrolyte at desired concentration. The sorption properties of this bentonite were reported elsewhere (Missana et al., 2008): clay cation exchange capacity (CEC) is 102 ± 4 meq/100 g and its N_2-BET specific area 33 $m^2\,g^{-1}$.

Aluminium oxide (γ-Al_2O_3) nanoparticles (Aldrich), with a nominal diameter lower than 50 nm and N_2-BET specific surface area of 136 $m^2\,g^{-1}$, were used. Characterisation details can be found elsewhere (Missana et al., 2014).

Suspensions of γ-Al_2O_3 and Na-smectite/γ-Al_2O_3 (S/A) mixtures were prepared at different weight fractions of fixed solid concentration (0.5 g L^{-1}), in $NaClO_4$ at variable ionic strength ($1{\cdot}10^{-2}$ M to $2{\cdot}10^{-1}$ M).

Radioactive isotope ^{85}Sr (Perkin Elmer) was used for sorption experiments. The carrier-free $^{85}SrCl_2$ solution (1 μM) was dissolved in 0.5 M HCl. ^{85}Sr is a gamma emitter (detected at 514 keV) with a half-life of 64.84 days. Sr activity in solution was measured by γ-counting with a NaI detector (Packard Auto-gamma COBRA 2). Non-radioactive $SrCl_2$ (Aldrich) solutions were used to achieve higher Sr concentrations.

2.2. Solid dissolution and equilibrium solutions

The solution in equilibrium with Na-smectite or γ-Al_2O_3 was analysed to determine the concentration of dissolved ions that may affect Sr speciation and/or sorption.

Suspensions were prepared in $1{\cdot}10^{-1}$ M $NaClO_4$ at different pH and were kept in contact for from 1 to 7 days. Samples were centrifuged and the supernatant was extracted and filtered (0.2 μm syringe filters) to determine the concentration of dissolved ions by chemical analyses. Trace elements were analysed by Inductively Coupled Plasma Atomic Emission Spectrometry (Varian 735 ES, AA240 FS). Anions were analysed by Ion Chromatography (DIONEX ICS-2000). The average concentrations measured for major anions and cations were included in speciation calculations and sorption modelling.

2.3. Sr sorption experiments

Strontium sorption on Na-smectite was previously analysed in (Missana and Garcia-Gutierrez, 2007; Missana et al., 2008). Equivalent experimental conditions were selected for Sr sorption studies on γ-Al_2O_3 and S/A mixtures.

Sorption experiments were carried out in 12 mL polypropylene centrifuge tubes, with a solid concentration of 0.5 g L^{-1}, under atmospheric conditions and at room temperature. Experiments were carried out in $NaClO_4$ at several ionic strengths and pH, which are set by adding aliquots of HCl or NaOH. To maintain pH constant over time, the buffer solutions indicated in Missana et al. (2009), were added at a concentration of $2{\cdot}10^{-3}$ M. Some experiments were carried out without buffers to verify that they did not interfere in Sr sorption.

On γ-Al_2O_3, Sr sorption kinetics was analysed at pH 6.5 in $1{\cdot}10^{-1}$ M $NaClO_4$ with a Sr concentration of $4.6{\cdot}10^{-6}$ M, from 5 min up to 3 months. Sorption edges were carried out, as a function of pH (3–11), at

different ionic strengths (from $1{\cdot}10^{-2}$ M to $2{\cdot}10^{-1}$ M) in $NaClO_4$ considering two Sr concentrations ($9.5{\cdot}10^{-9}$ M and $5{\cdot}10^{-6}$ M). The comparison of sorption edges at two different Sr concentrations allowed identifying additional sorption sites. Sorption isotherms on alumina were carried out in $1{\cdot}10^{-1}$ M $NaClO_4$ at pH 7.5 under varying Sr concentration (from $1{\cdot}10^{-10}$ to $1{\cdot}10^{-3}$ M).

Sr sorption on S/A mixtures was analysed in two ways. First, Sr sorption was evaluated, as a function of pH, on mixtures at different weight fractions (50S/50A and 20S/80A) in $NaClO_4$ at different ionic strengths ($1{\cdot}10^{-2}$ and $1{\cdot}10^{-1}$ M), with a Sr concentration of $9{\cdot}10^{-9}$ M. Second, Sr uptake was also evaluated on S/A mixtures, where alumina content in smectite increased from 0 to 100 wt %., with a Sr concentration of $9{\cdot}10^{-9}$ M, in $NaClO_4$ at two different ionic strengths ($1{\cdot}10^{-2}$ and $1{\cdot}10^{-1}$ M) and at two fixed pH (pH ≈ 4 and 9).

Kinetic studies showed that Sr sorption equilibrium was fast (Mayordomo, 2017) but all samples were maintained under stirring for seven days to replicate the conditions of previous studies (Missana and Garcia-Gutierrez, 2007; Missana et al., 2008). Afterwards, tubes were centrifuged at 14000 rpm for 1 h (21500 g). Aliquots of supernatant (2 mL) were extracted to measure Sr activity in solution. Measurements were done in triplicate and the errors in the activity measurements were lower than a 1%. The remaining solution was used to measure the pH. Sr(II) distribution coefficients (K_d) were calculated as:

$$K_d = \frac{C_i - C_{eq}}{C_{eq}}\frac{V}{m} = \frac{C_{ads}}{C_{eq}}\frac{V}{m} \quad (1)$$

where K_d is the distribution coefficient (mL·g^{-1}), C_i is the initial Sr(II) concentration (Bq·mL^{-1}), C_{eq} is the Sr(II) concentration measured in solution at equilibrium (Bq·mL^{-1}) and C_{ads} is the Sr(II) concentration sorbed, V is the suspension volume (mL) and m is the mass of sorbent (g). Sr sorption on centrifuge tubes was evaluated, being nearly negligible.

2.4. Al^{3+} competition with Sr^{2+} for cation exchange sites on smectite

To evaluate the possible competition of Al^{3+} ions with Sr^{2+} for cation exchange sites on Na-smectite, Sr sorption experiments were carried out with Na-smectite in $1{\cdot}10^{-2}$ M $NaClO_4$ at pH 4, with different Al^{3+} concentrations, by the addition of known concentrations of Al $(ClO_4)_3{\cdot}8H_2O$ (Aldrich). Experimental data will be used to determine γ-Al_2O_3 formation constant and Al^{3+} selectivity coefficient for Na-smectite cation exchange sites.

2.5. Sorption modelling

Strontium sorption on S/A mixtures was described considering sorption models (SMs) developed for the pure solids (Table 2), by an additive approach and just accounting for their weight fractions. The chemistry of water in equilibrium with the mixtures was incorporated.

The geochemical code CHESS 2.4 (Chemical Equilibrium of Species and Surfaces) was used for model calculations (van der Lee and de Wint, 1999). CHESS code has a thermodynamic framework to solve, through mass balance equations at the equilibrium, multicomponent speciation and surface reactions describing surface complexes. Strontium thermodynamic database of the French National Radioactive Waste Management Agency (ANDRA) (Giffaut et al., 2014) was used. Strontium aqueous and solid species and their corresponding formation constants are included in Table 1.

2.5.1. Sr sorption model on smectite

The sorption model selected to describe Sr sorption on Na-smectite was developed in (Missana and Garcia-Gutierrez, 2007). It included cation exchange and one-site non-electrostatic surface complexation. The surface complexation constants and solid parameters are collected in Table 2.

Table 1
Sr(II) thermodynamic database (Giffaut et al., 2014).

Species	Composition	log K
Aqueous		
Sr^{2+}	Basis species	
$SrCO_3$(aq)	1 Sr^{2+}, 1 HCO_3^-,-1 H^+	−7.519
$SrHCO_3^+$	1 Sr^{2+}, 1 HCO_3^-	1.181
$SrCl^+$	1 Sr^{2+}, 1 Cl^-	0.23
$SrOH^+$	1 Sr^{2+}, 1 H_2O, −1 H^+	−13.29
Solid		
$Sr(OH)_2$	1 Sr^{2+}, 2 H_2O, −2 H^+	−27.52
$SrCl_2$	1 Sr^{2+}, 2 Cl^-	−8.12
$SrCl_2{:}H_2O$	1 Sr^{2+}, 2 Cl^-, 1 H_2O	−4.91
$SrCl_2{:}2H_2O$	1 Sr^{2+}, 2 Cl^-, 2 H_2O	−3.49
$SrCl_2{:}6H_2O$	1 Sr^{2+}, 2 Cl^-, 6 H_2O	−1.61
SrO	1 Sr^{2+}, 1 H_2O, −2 H^+	−41.98
Strontianite ($SrCO_3$(s))	1 Sr^{2+}, 1 HCO_3^-,-1 H^+	−1.059

Table 2
Parameters and reactions used to describe Sr surface complexation on Na-smectite and γ-Al_2O_3. (1) (Missana and Garcia-Gutierrez, 2007); (2) (Missana et al., 2014); (3) (Mayordomo et al., 2016); (4) (Mayordomo, 2017); (*)this study.

Parameter	Na-smectite	γ-Al_2O_3
CEC (meq·100 g^{-1})	102 ± 4 (1)	
[S^wOH] (μeq·m^{-2})	1.82 (1)	1.1 (2)
[S^sOH] (μeq·m^{-2})	–	0.0095 (4)
BET (m^2·g^{-1})	33 (1)	136 (2)
Species and reactions	**Na-smectite log K**	**γ-Al_2O_3 log K**
Surface sites		–
$S^wOH + H^+ \rightleftharpoons S^wOH_2^+$	5.3 (1)	6.90 (2)
$S^wOH - H^+ \rightleftharpoons S^wO^-$	−8.4 (1)	−9.7 (2)
$S^sOH + H^+ \rightleftharpoons S^sOH_2^+$	–	6.90 (4)
$S^sOH - H^+ \rightleftharpoons S^sO^-$	–	−9.7 (4)
Sr sorption by cation exchange		
$2(Na \equiv X) + Sr^{2+} \rightleftharpoons (\equiv X)_2Sr + 2Na^+$	0.67 (1)	–
Sr sorption by surface complexation		
$S^wOH + Sr^{2+} \rightleftharpoons S^wO - Sr^+ + H^+$	−5.2 (1)	−4.8 (*)
$S^sOH + Sr^{2+} \rightleftharpoons S^sO - Sr^+ + H^+$	-	−2.3 (*)
Empirical Sr sorption	–	Log Kd (mL·g^{-1}) ≈ 2
Anion sorption on alumina		
$S^{w,s}OH + H^+ + HCO_3^- \rightleftharpoons S^{w,s}OH_2HCO_3$	–	11.2 (2)
$S^{w,s}OH + H^+ + ClO_4^- \rightleftharpoons S^{w,s}OH_2ClO_4$	–	8.5 (2)
$S^{w,s}OH + H^+ + Cl^- \rightleftharpoons S^{w,s}OH_2Cl$	–	9.2 (3)

Smectite has a layered structure consisting of two tetrahedral silicon sheets sandwiching an octahedral aluminium sheet, type 2:1 TOT (Grim, 1962), which exhibits a permanent negative charge as result of isomorphic substitution of Al and Si by lower valence cations. This charge is balanced by counter ions located in the interlayers which are available to be exchanged, giving the clay its cation exchange capacity (CEC). Cation exchange is the main sorption mechanism in smectite and its general formulation is:

$$z_BA \equiv X + z_AB^{z_B+} \overset{{}^B_AK_C}{\Leftrightarrow} z_AB \equiv X_{z_B} + z_BA^{z_A+} \quad (2)$$

where $\equiv X$ is the exchange site of a cation A with valence z_A (in this case, Na^+) that can be exchanged with cation B of valence z_B present in solution. ${}^B_AK_C$ is the selectivity coefficient defined, according to Gaines-Thomas expression, as:

$${}^B_AK_C = \frac{(N_B)^{Z_A}\{\gamma_A\}^{z_B}}{(N_A)^{Z_B}\{\gamma_B\}^{z_A}} \quad (3)$$

where γ_A and γ_B are the activities of the cations A and B, and N_A and N_B are their fractional occupancies on the solid, expressed as equivalents sorbed per mass of solid, $m_{sorbent}$, divided by the CEC, expressed in equivalents per mass

unit. When the concentration of *A* is much higher than the concentration of *B*, ${}^{B}_{A}K_{C}$ can be experimentally determined with the measured distribution coefficients (K_d).

An expression to determine ${}^{B}_{A}K_{C}$ experimentally was proposed in Bradbury and Baeyens (1994). When the concentration of cation A, [A], is much higher than the concentration of cation B, ${}^{B}_{A}K_{C}$ can be approximated to:

$$ {}^{B}_{A}K_{C} = \left(\frac{K_D \cdot Z_B}{CEC}\right)^{Z_A} \frac{\{\gamma_A\}^{Z_B}}{\{\gamma_B\}^{Z_A}} [A]^{Z_B} \quad (4) $$

where γ_A and γ_B are the activity coefficients of cations A and B, which are calculated using the Davies approximation, used for ionic strengths, I, with values $I \leq 0.5$ M:

$$ \log \gamma_i = [A] z_i^2 \left[\frac{\sqrt{I}}{1+\sqrt{I}} - 0.3I\right] \quad (5) $$

The direct use of selectivity coefficients in the geochemical code is not possible. To obtain the value incorporated in the code, K_{EX}, the following equation was proposed (Bradbury ad Baeyens, 1994):

$$ K_{EX} = \frac{(N_B)^{Z_A} \cdot \{\gamma_A\}^{Z_B}}{(N_A)^{Z_B} \cdot \{\gamma_B\}^{Z_A}} \quad (6) $$

where the concentration of cations A and B on the solid (N_A and N_B) and the activities in the liquid phase (γ_A and γ_B) are taken into account (Bradbury and Baeyens, 1994).

In Missana and Garcia-Gutierrez (2007), the competition of other cations present in solution was not accounted for because they did not improve the fit. However, in the mixtures, the competition of other cations in solution (Ca^{2+} and Al^{3+}) for cation exchange sites in smectite was considered. Their exchange reactions in smectite can be described with Eq. (2), with their corresponding selectivity coefficient, ${}^{B}_{A}K_{C}$. For Ca^{2+} a $\log {}^{Ca}_{Na}K_{C} = 0.65$ was considered (Missana and Garcia-Gutierrez, 2007) while Al^{3+} selectivity coefficient was here determined.

Sr complexation on surface hydroxyl edge sites (SOH) in smectite was also included. SOH sites have amphoteric behaviour (Sposito et al., 1999) and their protonation and deprotonation expressions are:

$$ SOH + H^+ \overset{K_+}{\Leftrightarrow} SOH_2^+ \quad (7) $$

$$ SOH \overset{K_-}{\Leftrightarrow} SO^- + H^+ \quad (8) $$

where K_+ and K_- are the protonation and deprotonation equilibria constants, respectively. These constants were determined by potentiometric titrations elsewhere (Missana and Garcia-Gutierrez, 2007) and their parameters are in Table 2.

Sr complexation on surface hydroxyl sites can occur by different mechanisms: inner- and outer-sphere complexation and also by ternary complexation with ions or ligands present in solution. In Na-smectite, only one type of surface site was considered, because sorption isotherms were linear and the presence of additional sorption sites was not identified. Sr^{2+} retention was described considering non-electrostatic inner-sphere complexation of the main species in solution (Sr^{2+}), with the following reaction:

$$ SOH + Sr^{2+} \overset{K_1}{\Leftrightarrow} SOSr^+ + H^+ \quad (9) $$

where K_1 is the equilibrium constant.

2.5.2. Sr sorption model on γ-Al_2O_3

Contaminant sorption on γ-Al_2O_3 takes place on surface hydroxyl groups (SOH) (Huang and Stumm, 1973). Two sorption sites, with different sorption affinity, named as weak (w) and strong (s) were considered. Their protonation reactions would be equivalent to those described in Eq. (7) and (8). The concentration of weak S^wOH sites and their protonation constants available of selected γ-Al_2O_3 were measured in Missana et al. (2014). The concentration of strong S^sOH sites and their constants were determined in (Mayordomo, 2017). The site parameters are included in Table 2.

For the sake of simplicity, to facilitate the modelling of mixtures, a non-electrostatic surface complexation model was selected as well to describe Sr sorption on γ-Al_2O_3, to facilitate the mixtures modelling. Titration data could be adequately reproduced with this approach (Missana et al., 2014).

Sr complexation on γ-Al_2O_3 surface sites (weak and strong) was described in the same way as for smectite, with (Eq. (9)).

The complexation of major anions present in solution (Cl^-, ClO_4^- or HCO_3^-) on positively charged surface weak and strong sites ($S^{w,s}OH_2^+$) was included in the model, considering their complexation on positively charged surface sites, with the following complexes (Missana et al., 2014):

$$ SOH_2^+ + HCO_3^- \overset{K_3}{\Leftrightarrow} SOH_2HCO_3 \quad (10) $$

$$ SOH_2^+ + ClO_4^- \overset{K_4}{\Leftrightarrow} SOH_2ClO_4 \quad (11) $$

$$ SOH_2^+ + Cl^- \overset{K_5}{\Leftrightarrow} SOH_2Cl \quad (12) $$

where K_i represent the complexation constants reported in Missana et al. (2014) and in Mayordomo et al. (2016).

3. Results

3.1. Chemical characteristics of equilibrium solutions and strontium speciation

The concentration of major anions and cations present in the supernatant was analysed. Regarding anions, ClO_4^-, HCO_3^- were identified in equilibrium solutions: the concentration of ClO_4^- comes from the electrolyte solution ($1{\cdot}10^{-2}$ M or $1{\cdot}10^{-1}$ M) and carbonate concentration comes from CO_2(g) equilibria and, in the case of Na-smectite, from salt and impurities dissolution. Measured HCO_3^- concentration ranges from 25 to 80 mg L^{-1} ($4.1{\cdot}10^{-4}$ M to $1.3{\cdot}10^{-3}$ M). A Cl^- concentration of $2.5{\cdot}10^{-3}$ M, coming from the addition of $^{85}SrCl_2$ tracer solution prepared in 0.5 M HCl, has been accounted for.

The main cations present in equilibrium solutions were Na^+, Ca^{2+} and Al^{3+}. Na^+ concentration is given by the electrolyte ($1{\cdot}10^{-2}$ M or $1{\cdot}10^{-1}$ M). For Na-smectite, Ca^{2+} was the main cation found in solution with an average concentration of $5{\cdot}10^{-5}$ M, while for γ-Al_2O_3 just Al^{3+} is found, due to alumina dissolution. Al^{3+} concentration was highly dependent on pH, and its relevance in Sr sorption in S/A mixtures was analysed.

Sr speciation was calculated considering a Sr concentration of $1{\cdot}10^{-6}$ M and the aqueous and solid species included in Table 1 (Giffaut et al., 2014). Sr speciation is mostly affected by chloride and carbonate ions (Felmy et al., 1998; Powell et al., 2011) and calculations were carried out considering atmospheric conditions and including the Cl^- concentration ($2.5{\cdot}10^{-3}$ M) equivalent to that of sorption experiments.

Under experimental conditions, Sr^{2+} is the main chemical species in solution (100%–95% from pH 3 to 9), $SrCl^+$ is below 0.1% and for pH > 9, carbonate aqueous complexes start to be relevant ($SrCO_3$(aq) and $SrHCO_3^+$), their contribution being below 5% of total strontium. For pH > 11, the concentration of strontium aqueous hydroxide ($SrOH^+$) starts to become appreciable. At low strontium concentration, no precipitation was predicted but, strontianite ($SrCO_3$(s)) is expected to limit Sr solubility under alkaline conditions with Sr concentration higher than $2{\cdot}10^{-3}$ M.

3.2. Sr sorption on Na-smectite

Experimental data of Sr sorption onto Na-smectite were taken from Missana and Garcia-Gutierrez, (2007). The main results and selected sorption model are summarised to facilitate the comparison with Sr

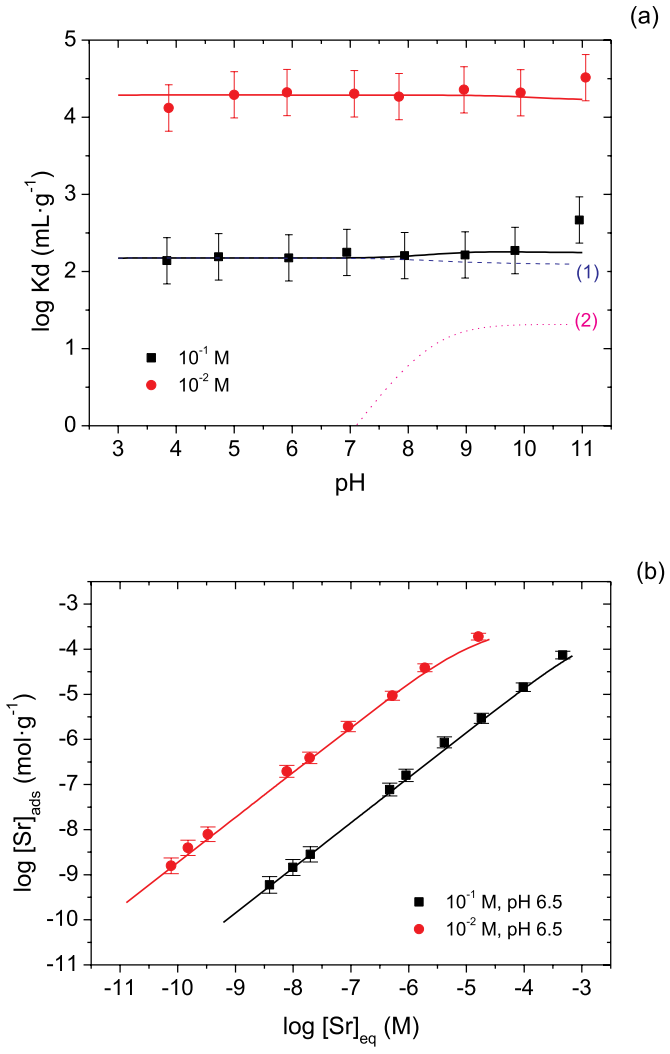

Fig. 1. Sr sorption on Na-smectite (4 g L^{-1}) in $NaClO_4$ at ionic strength: (■) 10^{-1} M and (●) 10^{-2} M. **(a)** Sorption edge with [Sr] = $1.6{\cdot}10^{-6}$ M; **(b)** Sorption isotherms at pH 6.5. Fits are plotted as continuous lines and the contribution of Sr complexes is indicated: (1) $Sr{\equiv}X_2$ and (2) $SO{-}Sr^+$. Data and model taken from (Missana and Garcia-Gutierrez, 2007).

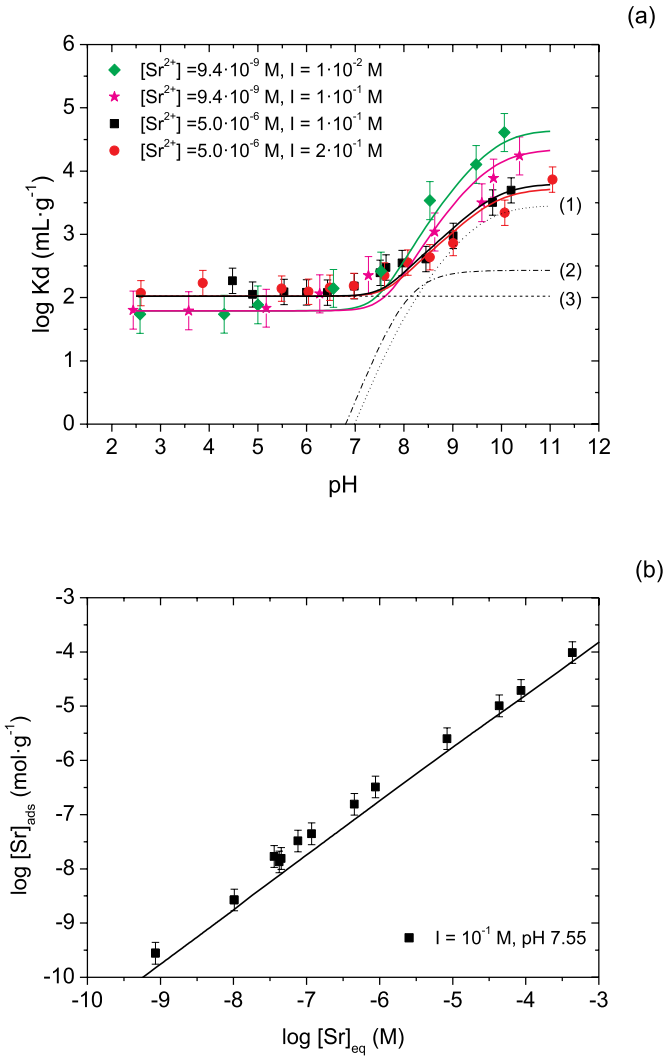

Fig. 2. (a) Sr sorption on γ-Al_2O_3 in $NaClO_4$ as a function of pH, varying ionic strength (I) and Sr concentration. **(b)** Sr(II) sorption isotherm on γ-Al_2O_3 (0.5 g L^{-1}) in $1{\cdot}10^{-1}$ M $NaClO_4$ at pH 7.5. Fits are plotted as continuous lines. The contribution of Sr complexes is indicated: (1) $S^wO\text{-}Sr^+$, (2) $S^sO\text{-}Sr^+$, (3) Empirical log Kd (mL·g^{-1}) = 2.

sorption experiments obtained in γ-Al_2O_3 (A) and in the S/A mixtures.

Kinetic studies showed that Sr sorption was fast and equilibrium was reached in few hours. Fig. 1a shows Sr distribution coefficients measured on Na-smectite as a function of pH at different ionic strengths. Fig. 1b shows Sr sorption isotherms, obtained at pH 6.5 and at two ionic strengths. Sr sorption onto Na-smectite increased with decreasing ionic strength and it was mainly independent of pH, indicating cation exchange as the main Sr sorption mechanism. Only at pH > 9, a small contribution of Sr complexation on negatively charged edge sites was appreciated. Sorption was linear over a wide range of Sr concentrations ($1{\cdot}10^{-9}$ to $1{\cdot}10^{-4}$ M) (Fig. 1b).

The output of the model proposed to describe Sr sorption on Na-smectite is plotted as continuous lines in Fig. 1a and b. Cation exchange with Na^+ ($Sr{\equiv}X_2$) is indicated in Fig. 1a as (1) (selectivity coefficient ($^{Sr}_{Na}K_C$) of log $^{Sr}_{Na}K_C$ = 0.7, Eq. (2)) (Missana and Garcia-Gutierrez, 2007). Sr sorption over pH 9, was described with complexation of the main aqueous species in solution (Sr^{2+}) with SO^- surface sites ($SO{-}Sr^+$, Eq. (9)) and it is indicated as (2) in Fig. 1a. The model reactions and constants are included in Table 2. Sr experimental data was adequately reproduced by the model, only for pH > 11 the model under predicted measured log Kd. Some Sr precipitation cannot be ruled out.

3.3. Sr sorption on γ-Al_2O_3

Strontium sorption kinetics was analysed onto γ-Al_2O_3 at pH 6.5. The distribution coefficients measured after 5 min and up to 3 months were the same, indicating fast kinetics (Mayordomo, 2017).

Fig. 2a shows Sr distribution coefficients measured on γ-Al_2O_3 as function of pH, in $NaClO_4$ at different ionic strengths ($1{\cdot}10^{-2}$ M, $1{\cdot}10^{-1}$ M and $2{\cdot}10^{-1}$ M) and Sr concentrations ($9.5{\cdot}10^{-9}$ M and $5{\cdot}10^{-6}$ M). Fig. 2b presents Sr sorption isotherm measured at pH 7.5 in $1{\cdot}10^{-1}$ M $NaClO_4$ with Sr concentration from $1{\cdot}10^{-9}$ M to $1{\cdot}10^{-3}$ M.

Strontium sorption was independent of ionic strength but dependent on pH, varying from 5% (pH 3–5) up to 95% strontium uptake, as expected for cation sorption on an oxide (Dzombak and Morel, 1990). Sorption edges obtained with different initial Sr concentration suggested the existence of two sorption sites, since sorption is higher at lower Sr concentration, especially at high pH. In all studied cases, for pH < 7, a non-null Sr sorption plateau is observed (log $K_d \approx 2$, mL·g^{-1}), mostly independent of pH or ionic strength.

A two-site non-electrostatic model was proposed for γ-Al_2O_3. All model parameters, reactions and constants are in Table 2. The sorption of anions present in solution (Cl^-, ClO_4^-, HCO_3^-) on both weak and

strong sites was incorporated into the model.

Sr sorption was modelled considering inner-sphere complexation of Sr^{2+} ($SO{-}Sr^{+}$) on weak and strong sites (Eq. (10)). The individual contributions of $SO{-}Sr^{+}$ complexes are respectively indicated as (1) and (2) in Fig. 2. These complexes adequately described measured Sr sorption onto γ-Al_2O_3 for pH > 7.5, but did not account for sorption measured at lower pH.

Under acid to neutral pH, Sr sorption represents a retention around a 5%. This Sr sorption was unexpected, because for pH lower than the point of zero charge (pH_{PZC} = 8.3) of γ-Al_2O_3, surface sites are positively charged (SOH_2^{+}) and its interaction with Sr^{2+} should be hindered. However, in this material, Sr sorption was systematically measured within the acid pH region, independently of the pH or ionic strength. The same behaviour was observed for other cations, such as Cd^{2+} or UO_2^{2+} (Mayordomo, 2017).

Since we want to describe Sr sorption in S/A mixtures by an additive model, we necessarily need to adequately fit Sr sorption under all conditions.

We hypothesized that certain anions, which were already retained on γ-Al_2O_3 surface (Hingtson et al., 1967; Missana et al., 2014) may enhance Sr uptake. Similarly, an increase of Sr retention on goethite in presence of sorbing anions has been recently reported (Nie et al., 2017). Some authors considered the formation of weak ion pairs involving anions and surface hydroxyl groups (Yates et al., 1973) or strong specific adsorption (Szczepaniak and Koscielna, 2002). Another cases considered that these ions are not specifically sorbed on the surface, but they are actually held at the surface by electrostatic forces to balance the surface charge (Breeuwsma and Lyklema, 1973). Co-precipitation with some aluminate phase could also explain this behaviour.

To date, no experimental evidence is available to reliably define the complex that promotes cation sorption in γ-Al_2O_3 surface at acidic pH. For this reason, and to maintain the rigour in the definition of the non-electrostatic model, we decided to include the empirical sorption (log Kd ($mL{\cdot}g^{-1}$) ≈ 2) in the model. The contribution is indicated in Fig. 2a as (3). The model (Table 2) described the whole experimental data and the behaviour with pH, ionic strength and with initial strontium load (Fig. 2). The model predicts strontianite precipitation for Sr concentration higher than $1{\cdot}10^{-3}$ M.

3.4. Sr sorption in Na-smectite/γ-Al_2O_3 (S/A) mixtures

Considering the different Sr sorption behaviour exhibited by Sr on smectite (dominated by cation exchange and ionic strength dependent) and on γ-Al_2O_3 (by surface complexation and pH dependent), Sr sorption on S/A mixtures was evaluated as a function of pH, at two different ionic strengths (I).

Fig. 3 shows Sr sorption edges measured in two S/A mixtures (50S/50A and 20S/80A) at I = $1{\cdot}10^{-1}$ M (Fig. 3a) and I = $1{\cdot}10^{-2}$ M (Fig. 3b). Sr sorption edges measured on Na-smectite (100 S) and γ-Al_2O_3 (100 A) are included for comparison. It can be seen that Sr sorption on S/A mixtures is highly affected by ionic strength, pH, and by the ratio of the two sorbents. The effect of mixture composition on Sr sorption was analysed more in detail. Fig. 4 shows Sr sorption on S/A mixtures with increasing γ-Al_2O_3 content (wt. %), measured at different pH (pH 4 and 9) at I = $1{\cdot}10^{-1}$ M (Figs. 4a) and $1{\cdot}10^{-2}$ M (Fig. 4b).

In the figures, dashed and dotted lines are the fits considering the additive sorption model (SM) (Table 2). At high ionic strength ($1{\cdot}10^{-1}$ M) (Fig. 3a), Sr sorption in S/A mixtures varied with pH. For pH < 7, Sr sorption is the same (log Kd = 2 $mL\,g^{-1}$) in Na-smectite and in γ-Al_2O_3. However, for pH > 7, the addition of γ-Al_2O_3 to smectite enhances Sr sorption from log Kd ($mL{\cdot}g^{-1}$) = 2 to log Kd ($mL{\cdot}g^{-1}$) = 3, because of the higher Sr affinity towards γ-Al_2O_3. With the addition of only 20 wt % γ-Al_2O_3 to Na-smectite the sorption capacities of pure γ-Al_2O_3 are almost achieved (Fig. 4a). Other mixtures of smectite with zeolite (Başçetin and Atun, 2010) or illite (Missana et al., 2008) showed improved Sr sorption under specific conditions.

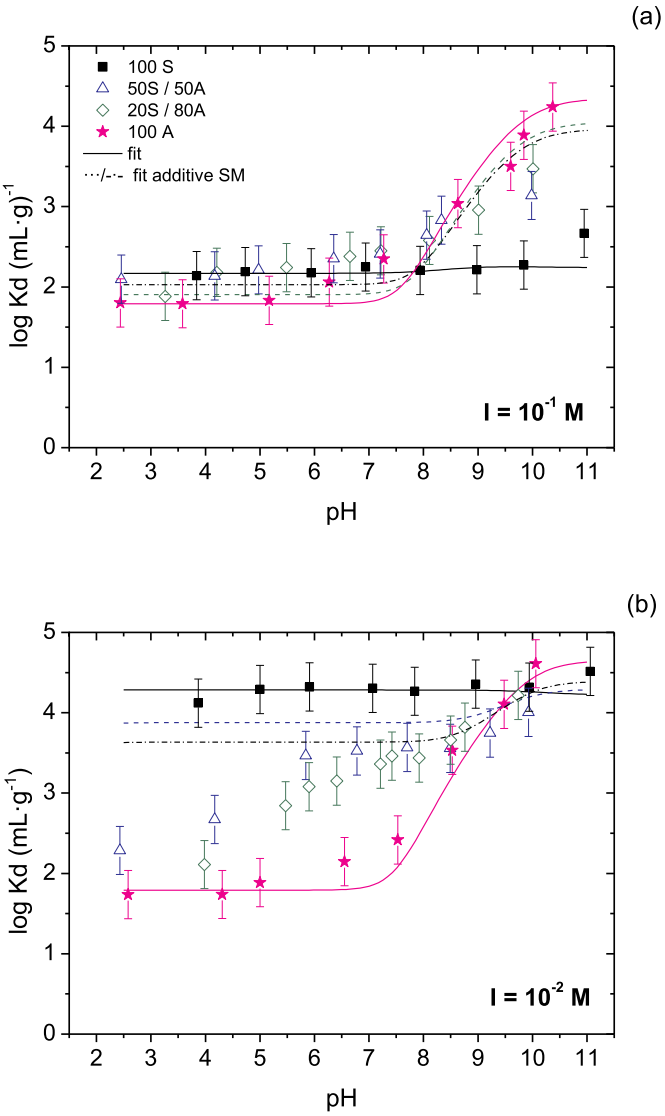

Fig. 3. Sr distribution coefficients measured on (■) Na-smectite (100 S), (★) γ-Al_2O_3 (100A), (△) Mixture 50 S/50A and (◇) Mixture 20S/80A with 0.5 g L^{-1}, as a function of pH in $NaClO_4$ at ionic strength (I): **(a)** $1{\cdot}10^{-1}$ M and **(b)** $1{\cdot}10^{-2}$ M. Continuous lines are fits of the individual systems and dashed (50S/50A) and dotted (20S/80A) lines are the fits using the additive sorption model (SM) (Table 2).

The fits considering the additive SM are plotted as dashed and dotted lines in Figs. 3 and as continuous lines in Fig. 4. It can be seen that, at $1{\cdot}10^{-1}$ M ionic strength, Sr sorption in S/A mixtures was satisfactorily modelled, indicating that sorption is additive (Figs. 3a and 4a).

At lower ionic strength ($1{\cdot}10^{-2}$ M) Sr sorption behaviour in S/A mixtures was again dependent on pH (Fig. 3b). For pH > 9, Sr is sorbed by surface complexation both in Na-smectite and γ-Al_2O_3 (log Kd ($mL{\cdot}g^{-1}$) ≈ 4) and Sr sorption in the mixtures did not vary with the γ-Al_2O_3 content (Fig. 4b). However, at $1{\cdot}10^{-2}$ M and pH < 9, Sr sorption in Na-smectite is dominated by cation exchange and it is higher than in γ-Al_2O_3 (Fig. 3b). Again, Sr sorption in S/A mixtures was simulated with the additive SM (fits are plotted as continuous lines in Fig. 3b). At ionic strength $1{\cdot}10^{-2}$ M and alkaline pH conditions, Sr sorption in mixtures is adequately reproduced. However, for I = $1{\cdot}10^{-2}$ M and pH < 9, the model over-predicted Sr sorption and this effect was even more pronounced at acid pH (Fig. 3b). At I = $1{\cdot}10^{-2}$ M and pH 4, the model overestimation occurred at all mixture ratios analysed (Fig. 4b). For example, in the mixture with an

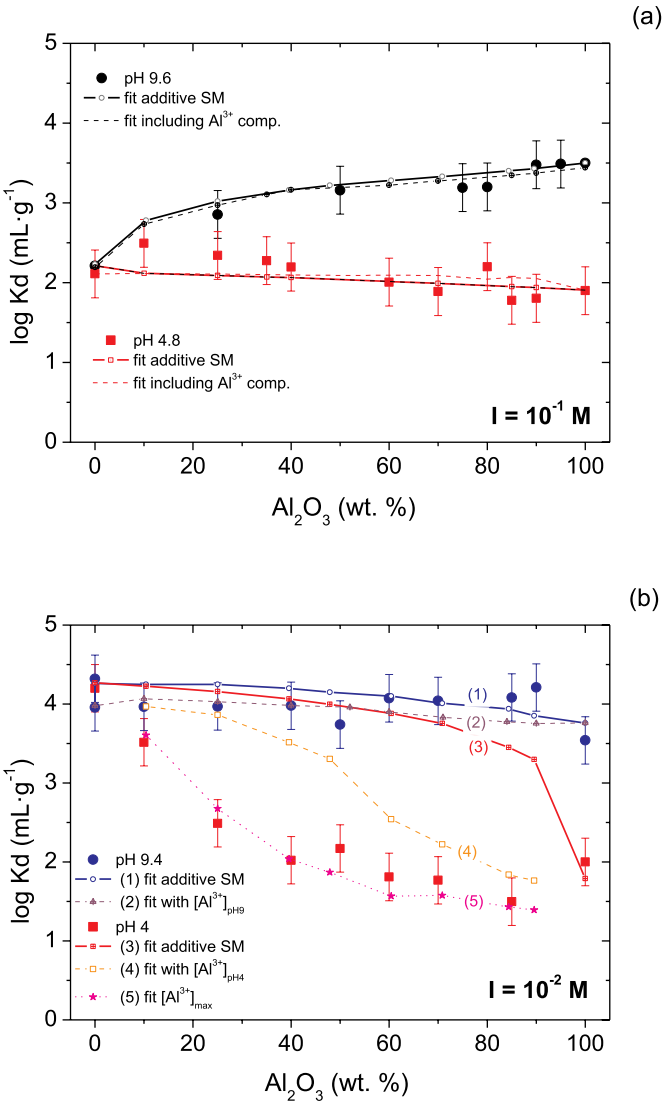

Fig. 4. Sr distribution coefficients on smectite with different γ- Al_2O_3 content (wt. %) at pH 4 or 9, in $NaClO_4$ **(a)** $1{\cdot}10^{-2}$ M and **(b)** $1{\cdot}10^{-1}$ M. Lines (1) & (3): Fits additive sorption model (SM); Lines (2) & (4): Fits considering Al^{3+} competition and measured $[Al^{3+}]_{pH9}$ and $[Al^{3+}]_{pH4}$; Line (5): Fit considering maximum $[Al^{3+}]_{max}$ concentration of 12 mg L^{-1}.

80% content of Al_2O_3 (20S/80A), measured log K_d was 2.5 mL g^{-1} and predicted log K_d was 3.8 mL g^{-1}.

As mentioned before, at low ionic strength and acid pH, cation exchange in smectite is the dominant sorption mechanism in the mixtures. The lack of fit under these conditions suggests that cation exchange in smectite is somehow affected by the presence of alumina. Other cations present in solution may compete with Sr for sorption sites reducing sorption (Kasar et al., 2017; Marinovic et al., 2017). This effect is more relevant at the low ionic strengths, when sorption by ionic exchange is favoured as the electrolyte ion concentration is decreased in respect to other potentially competing ions (McKinley et al., 2007). The competition of divalent cations coming from smectite dissolution (Ca^{2+}, Mg^{2+}, with a maximum concentration of $5{\cdot}10^{-5}$ M) was analysed in (Missana and Garcia-Gutierrez, 2007; Missana et al., 2008) and significant effect was discarded. Therefore, γ-Al_2O_3 presence in the mixtures must be responsible for the reduced Sr uptake in smectite. To analyse this possibility, we studied both γ-Al_2O_3 dissolution at different pH conditions and the competing effects of Al^{3+} ions with Sr for cation exchange sites in Na-smectite.

Fig. 5 plots the Al^{3+} concentration in equilibrium with γ-Al_2O_3 set

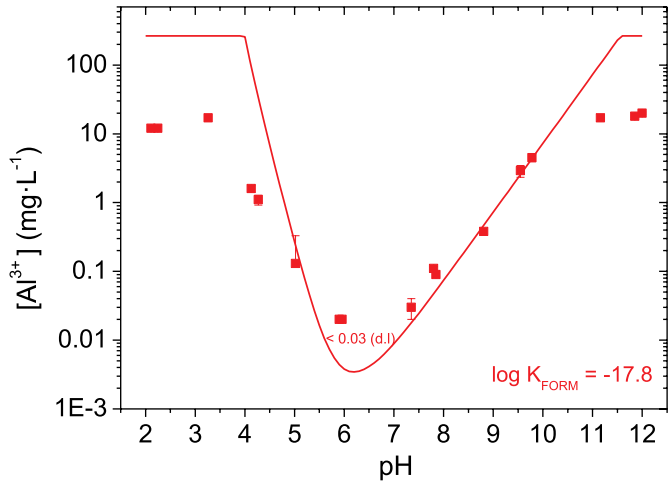

Fig. 5. Al^{3+} dissolved from γ-Al_2O_3 in $NaClO_4$ (0.5 g L^{-1} at $1{\cdot}10^{-1}$ M) as a function of pH. Detection limit (d.l.) = 0.03 mg L^{-1}. Fit considering a log K_{FORM} = −17.8 is plotted as a line.

at different pH for one week. The concentration of dissolved Al^{3+} is highly dependent on pH, ranging from values lower than 0.03 mg L^{-1} (detection limit, *d.l.*) at neutral pH values, up to maximum $[Al^{3+}]_{max} \approx 12$ mg L^{-1} at acid (pH = 2–3) or basic pH (pH = 11–12). The maximum Al^{3+} concentration measured corresponds to a solid dissolution lower than a 3.6%.

The equation defining alumina dissolution is:

$$2Al^{3+} + 3H_2O - 6H^+ \overset{K_{FORM}}{\rightleftarrows} Al_2O_3 \quad (13)$$

where K_{FORM} is the formation constant.

The fit of γ-Al_2O_3 dissolution is plotted as a line in Fig. 5. Al^{3+} speciation was incorporated considering the Al hydrolysis constants from NAGRA/PSI database (Thoegen et al., 2014). The required log K_{FORM} was −17.8, in the range of values reported for equivalent alumina phases (log K_{FORM} = −16.1 to −19.1) (Barin, 1995; Chen et al., 1995) where the higher values reported usually correspond to alumina phases obtained at high temperatures (Chase et al., 1974).

The competition of Al^{3+} ions with Sr^{2+} for cation sites in smectite was evaluated. Fig. 6 presents Sr distribution coefficients measured on

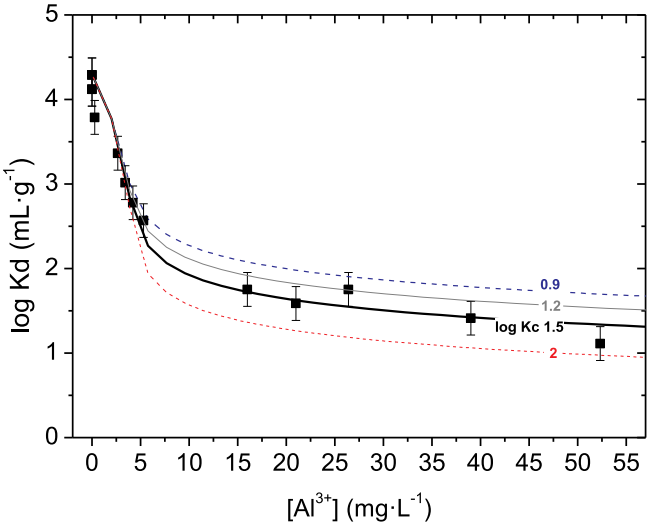

Fig. 6. Sr distribution coefficients measured on Na-smectite (0.5 g L^{-1}) in 10^{-2} M $NaClO_4$ with variable of Al^{3+} concentration in solution ([Sr] = $6\ 10^{-9}$ M). Lines are fits considering different Al^{3+} selectivity coefficients for Na-smectite (log ${}^{B}_{A}K_{C}$).

Na-smectite in 10^{-2} M $NaClO_4$ at pH 4 with different Al^{3+} concentrations. It can be seen that Sr distribution coefficients decreased abruptly when aluminium is added, from log Kd of 4.2 to log Kd of 1.8 mL g^{-1} with $[Al^{3+}] = 15$ mg L^{-1}. For higher Al^{3+} concentrations the decrease is smaller, being the log Kd reduced to 1 mL g^{-1} with $[Al^{3+}] = 50$ mg L^{-1}.

The selectivity coefficient of Al^{3+} for cation exchange sites in Na-smectite (Eq. (2)) was estimated by competition with Sr^{2+}, by fixing the Sr^{2+} selectivity coefficient for Na-smectite ($\log {}^{Sr}_{Na}K_C = 0.70$). As can be seen in Fig. 6, for Al^{3+} concentrations lower than 5 mg L^{-1}, the model is not very sensitive to Al^{3+} selectivity coefficient and $\log {}^{Al}_{Na}K_C$ values from 0.9 to 2.00 could fit data. However, at higher Al^{3+} concentrations, the best fit is achieved with a $\log {}^{Al}_{Na}K_C = 1.5$, a value within selectivity coefficients usually reported for trivalent cations in smectite: Log K_c from 1.4 to 2 (Bradbury and Baeyens, 2005).

Afterwards, Sr sorption data in S/A mixtures (Fig. 4) were re-simulated considering the competition of Al^{3+} ions. Simulations are done taking into account the Al^{3+} concentrations measured in solution (Fig. 6a) at studied pH and the obtained selectivity coefficient ($\log {}^{Al}_{Na}K_C = 1.5$). The fits are calculated in the mixtures point by point, modulating $[Al^{3+}]$ concentrations, plotted as dashed or dotted lines in Fig. 4.

In those cases where Sr sorption in the mixtures was already well described by the additive SM, the inclusion of the competition of Al^{3+} ions (plotted as dashed lines) did not significantly modify the SM predictions (plotted as continuous lines). This happened at high ionic strength at both pH analysed (Fig. 4a), and at low ionic strength and pH 9 (Fig. 4b), where cation exchange is less relevant.

However, at ionic strength 10^{-2} M and pH 4, additive SM overpredicted Sr sorption (line (3) in Fig. 4b). The new fit including Al^{3+} competition, considering measured $[Al^{3+}]_{pH4} = 2$ mg L^{-1}, is indicated as (4) in Fig. 4b. It is observed than when Al^{3+} competition is included, the fit predicts a decrease of Sr sorption, more relevant for alumina content > 50 wt %. Nevertheless, this assumption is not enough to represent the observed Sr sorption decrease under acid pH and low ionic strength conditions. In order to reproduce Sr sorption measured in the mixtures at pH 4 (fit indicated as line (5)), an Al^{3+} concentration six times higher ($[Al^{3+}]_{max} \approx 12$ mg L^{-1}) would be needed for, approaching the values measured at much lower pH (2–3). However, although pH and concentration determination have associated uncertainties, they are not expected to be that broad. As a consequence, the Al^{3+} competition with Sr^{2+} cannot fully explain the Sr sorption decrease in mixtures. This indicates that an additional process must inhibit Sr sorption in the mixture.

This is an interesting finding because complementary stability experiments showed that the addition of γ-Al_2O_3 to smectite causes fast (hetero)aggregation (Mayordomo et al., 2014, 2016; Mayordomo, 2017). Hence, it is possible that due to S/A heteroagregation phenomena, alumina nanoparticles interact with the smectite layers and hinder the access to available exchange sites in smectite. This result contrasts with the sorption behaviour of selenite on the same smectite/γ-Al_2O_3 mixtures, where selenite sorption was increased and where the additive model perfectly reproduced sorption data (Mayordomo et al., 2016). The fact that selenite and Sr are sorbed by different mechanisms on smectite, suggests that smectite and alumina interactions may hinder the access to cation exchange sites in smectite, an aspect that will be verified with other relevant contaminants.

4. Conclusions

Strontium sorption on Na-smectite/γ-Al_2O_3 (S/A) mixtures was analysed to analyse if the addition of alumina nanoparticles enhance sorption and to verify the applicability of a sorption model based on the component additive approach. The study was undertaken by analysing first Sr sorption on the pure solids as function of pH, ionic strength and Sr concentration, to provide thermodynamically–based sorption models (SMs).

Sr sorption in S/A mixtures was highly dependent on ionic strength and on pH. At high ionic strength and alkaline pH, Sr sorption by cation exchange in smectite is limited and the addition of alumina to smectite enhanced Sr retention. Under these conditions, where surface complexation dominated, the additive sorption model adequately reproduced Sr sorption in the S/A mixture. However, at low ionic strength and acid pH, where cation exchange mechanism is relevant, alumina did not have a positive effect on Sr retention. Furthermore, the additive model significantly overestimated Sr sorption in the mixture, suggesting that alumina presence hindered Sr sorption in smectite.

The possible competition of Al^{3+} ions, coming from alumina dissolution, for exchangeable sites in smectite was analysed and it partially, but not fully, explained the decrease on Sr sorption under acidic pH and low ionic strength. This suggested that alumina particles interaction with smectite layers may favour a charge shielding of smectite layers, limiting the cation access to exchangeable sites, an assumption to be verified with further studies.

Acknowledgments

This work has been supported by MIRAME Project (CTM2014-60482-P), granted by the Spanish Ministry of Economy and Competiveness. N.M acknowledges FPI BES-2012-056603 pre-doctoral grant from MINECO (Spain). The Chemistry Division of CIEMAT (Madrid, Spain) is acknowledged for the chemical analyses. We are grateful for the review made by two anonymous reviewers and by the Executive Editor, Prof. Michael Kersten, which significantly improved the manuscript.

References

Ahmadi, S.J., Akbari, N., Shiri-Yekta, Z., Mashhadizadeh, M.H., Hosseinpour, M., 2015. Removal of strontium ions from nuclear waste using synthesized MnO_2-ZrO_2 nanocomposite by hydrothermal method in supercritical condition. Kor. J. Chem. Eng. 32, 478–485.
Alessi, D.S., Fein, J.B., 2010. Cadmium adsorption to mixtures of soil components: testing the component additivity approach. Chem. Geol. 270 (1–4), 186–195.
Anderson, P.R., Benjamin, M.M., 1990. Surface and bulk characteristics of binary oxide suspensions. Environ. Sci. Technol. 24, 692–698.
Asztemborska, M., Jakubiak, M., Rykaczewska, M., Bembenek, M., St?borowski, R., Bystrzejewska-Piotrowska, G., 2016. Mycoextraction of radiolabeled cesium and strontium by Pleurotus eryngii mycelia in the presence of alumina nanoparticles: sorption and accumulation studies. J. Environ. Radioact. 164, 190–196.
Baeyens, B., Bradbury, M.H., 1997. A mechanistic description of Ni and Zn sorption on Na-montmorillonite Part I: titration and sorption measurements. J. Contam. Hydrol. 27, 199–222.
Barin, I., 1995. Thermochemical Data of Pure Substances, Third. Ed. VCH, Weinheim (Germany).
Basçetin, E., Atun, G., 2010. Adsorptive removal of strontium by binary mineral mixtures of montmorillonite and zeolite. J. Chem. Eng. Data 55, 783–788.
Bonner, W.P., Bevis, H.A., Morgan, J.J., 1966. Removal of strontium from water by activated alumina. Health Phys. 12, 1691–1703.
Bradbury, M.H., Baeyens, B., 1994. Sorption by Cation Exchange. Incorporation of a Cation Exchange Model into Geochemical Computer Codes. PSI Bericht Nr. 94-07. Nagra Report NTB 94-11 (Switzerland). .
Bradbury, M.H., Baeyens, B., 1997. A mechanistic description of Ni and Zn sorption on Na-montmorillonite. Part II: modelling. J. Contam. Hydrol. 27, 223–248.
Bradbury, M.H., Baeyens, B., 2005. Modelling the sorption of Mn(II), Co(II), Ni(II), Zn(II), Cd(II), Eu(III), Am(III), Sn(IV), Th(IV), Np(V) and U(VI) on montmorillonite: linear free energy relationships and estimates of surface binding constants for some selected heavy metals and actinide. Geochem. Cosmochim. Acta 69, 875–892.
Breeuwsma, A., Lyklema, J., 1973. Physical and chemical adsorption of ions in the electrical double layer on hematite (?-Fe2O3). J. Colloid Interface Sci. 43, 437–448.
Chase, M.W., Curnutt, J.L., Prophet, H., Syverud, A.N., Walker, L.C., 1974. JANAF thermochemical tables. J. Phys. Chem. Ref. Data 3, 311–480.
Chen, Q., Zeng, W., Chen, X., Gu, S., Yang, G., Zhou, H., Yin, Z., 1995. Investigation of the thermodynamic properties of γ-Al2O3. Termochimica Acta 253, 33–39.
Comarmond, M.J., Payne, T.E., Collins, R.N., Palmer, G., Lumpkin, G.R., Angove, M.J., 2012. Inhibition of uranium(VI) sorption on titanium dioxide by surface iron(III) species in ferric oxide/titanium dioxide systems. Environ. Sci. Technol. 46, 11128–11134.
Davis, J.A., Coston, J.A., Kent, D.B., Fuller, C.C., 1998. Application of the surface complexation concept to complex mineral assemblages. Environ. Sci. Technol. 32, 2820–2828.
Dzombak, D.A., Morel, F.M.M., 1990. Surface Complexation Modeling. Hydrous Ferric

Oxide. John Wiley and Sons, Cambridge (United States).
Felmy, A.R., Dixon, D., Rustad, J.R., Mason, M.J., Onishi, L.M., 1998. The hydrolysis and carbonate complexation of strontium and calcium in aqueous solution. Use of molecular modeling calculations in the development of aqueous thermodynamic models. J. Chem. Thermodyn. 30, 1103–1120.
Fuller, A.J., Shaw, S., Peacock, C.L., Trivedi, D., Burke, I.T., 2016. EXAFS study of Sr sorption to illite, goethite, chlorite, and mixed sediment under hyperalkaline conditions. Langmuir 32, 2937–2946.
Galamboš, M., Kuf?áková, J., Rosskopfová, O., Rajec, P., 2010. Adsorption of cesium and strontium on natrified bentonites. J. Radioanal. Nucl. Chem. 283, 803–813.
Giffaut, E., Grivé, M., Blanc, P., Vieillard, P., Colàs, E., Gailhanou, H., Gaboreau, S., Marty, N., Madé, B., Duro, L., 2014. Andra thermodynamic database for performance assessment: ThermoChimie. Appl. Geochem. 49, 225–236.
Grim, R.E., 1962. Applied Clay Mineralogy. Mc Graw-Hill, Toronto (Canada).
Hingston, F.J., Atkinson, R.J., Posner, A.M., Quirk, J.P., 1967. Specific adsorption of anions. Nature 215, 1459–1461.
Honeyman, B.D., Santschi, P.H., 1991. Coupling adsorption and particle aggregation-Laboratory studies of colloidal pumping using fe-59 labelled hematite. Environ. Sci. Technol. 25 (10), 1739–1747.
Hua, M., Zhang, S., Pan, B., Zhang, W., Zhang, Q., 2012. Heavy metal removal from water/wastewater by nanosized metal oxides: a review. J. Hazard Mater. 211–212, 317–331.
Huang, C.P., Stumm, W., 1973. Specific adsorption of cations on hydrous gamma-Al_2O_3. J. Colloid Interface Sci. 43, 409–420.
Huertas, F., Fuentes-Santillana, J.L., Jullien, F., Rivas, P., Linares, J., Fariña, P., Ghoreychi, M., Jockwer, N., Kickmaier, W., Martínez, M.A., Samper, J., Alonso, E., Elorza, F.J., 2000. Full Scale Engineered Barriers Experiment for a Deep Geological Repository for High-Level Radioactive Waste in Crystalline Host Rock. EC Final REPORT EUR 19147. .
IAEA, 2006. Environmental consequences of the Chernobyl accident and their remediation: twenty years of experience. In: Report of the Chernobyl Forum Expert Group 'Environment'. International Atomic Energy Agency Vienna, Austria, pp. 166.
Jeong, C.H., Kim, C.S., Kim, S.J., Park, S.W., 1996. Affinity of radioactive cesium and strontium for illite and smectite clay in the presence of groundwater ions. J. Environ. Sci. Heal. Part a-Environmental Sci. Eng. Toxic Hazard. Subst. Control. 31, 2173–2192.
Karamalidis, A.K., Dzombak, D., 2010. Surface Complexation Modeling Gibbsite. Wiley, New Jersey, USA.
Kasar, S., Kumar, S., Saha, A., Tomar, B.S., Bajpai, R.K., 2017. Mechanistic and thermodynamic aspects of Cs(I) and Sr(II) interactions with smectite-rich natural clay. Environ. Earth Sci. 76, 1–9.
Kasprzyk-Hordern, B., 2004. Chemistry of alumina, reactions in aqueous solution and its application in water treatment. Adv. Colloid Interface Sci. 110, 19–48.
Katz, L.E., Criscenti, L.J., Chen, C.C., Larentzos, J.P., Liljestrand, H.M., 2013. Temperature effects on alkaline earth metal ions adsorption on gibbsite: approaches from macroscopic sorption experiments and molecular dynamics simulations. J. Colloid Interface Sci. 399, 68–76.
Kayvani Fard, A., Mckay, G., Preud'Homme, H., Kochkodan, V., Atieh, M.A., 2017. Fabrication and evaluation of activated carbon/Fe_2O_3 nano-composite on the removal of strontium ions from water. Desalin. Water Treat. 73, 399–408.
Khin, M.M., Nair, A.S., Babu, V.J., Murugan, R., Ramakrishna, S., 2012. A review on Nanomaterials for Environmental remediation. Energy Environ. Sci. 5, 8075–8109.
Kinninburgh, D.G., Syers, J.K., Jackson, M.L., 1975. Specific adsorption of trace amounts of calcium and strontium by hydrous oxides of iron and aluminum. Soil Sci. Soc. Am. J. 39, 464–470.
Kohlicková, M., Jedináková-Kcižová, V., 1998. Effect of pH and Eh on the sorption of selected radionuclides. J. Radioanal. Nucl. Chem. 229, 43–48.
Kuiken, T., 2010. Cleaning up contaminated waste sites: is nanotechnology the answer? Nano Today 5, 6–8.
Landry, C.J., Koretsky, C.M., Lund, T.J., Lund, T.J., Schaller, M., Das, S., 2009. Surface complexation modeling of Co(II) adsorption on mixtures of hydrous ferric oxide, quartz and kaolinite. Geochem. Cosmochim. Acta 73, 3723–3737.
Lee, J.O., Lee, K.J., Cho, W.J., 1997. Sorption and diffusion of I-125 and Sr-90 in a mixture of bentonite and crushed granite backfill of a radioactive waste repository. Radiochim. Acta 76 143-15.
Li, T., He, F., Dai, Y., 2016. Prussian blue analog caged in chitosan surface-decorated carbon nanotubes for removal cesium and strontium. J. Radioanal. Nucl. Chem. 310, 1139–1145.
MacMillan, J.P., Park, J.W., R, G., Wagner, H., Köhler, K., Wallbrecht, P., 2000. Strontium and Strontium Compounds. Wiley-VCH.
Marinovic, S.R., Ajdukovic, M.J., Jovic-Jovicic, N.P., Mudrinic, T.M., Nedic-Vasiljevic, B.M., Bankovic, P.T., Milutinovic-nikolic, A.D., 2017. Adsorption of strontium on different sodium-enriched bentonites. J. Serb. Chem. Soc. 82, 449–463.
Mayordomo, N., 2017. Experimental and Theoretical Studies of Mixed Smectite and Al2O3 Nanoparticles to Improve Pollutant Retention in Geochemical Barriers. Doctoral Dissertation. Universidad de Alcalá de Henares, UAH, Madrid, Spain).
Mayordomo, N., Alonso, U., Missana, T., Benedicto, A., García-Gutiérrez, M., 2014. Addition of Al_2O_3 nanoparticles to bentonite: effects on surface charge and Cd sorption properties. In: Scientific Basis for Nuclear Waste Management XXXVII. Mat. Res. Symp. Proc, vol. 1665. pp. 131–138.
Mayordomo, N., Alonso, U., Missana, T., 2016. Analysis of the improvement of selenite retention in smectite by adding alumina nanoparticles. Sci. Total Environ. 572, 1025–1032.
McKinley, J.P., Zachara, J.M., Smith, S.C., Liu, C., 2007. Cation exchange reactions controlling desorption of 90Sr2+ from coarse-grained contaminated sediments at the Hanford site, Washington. Geochem. Cosmochim. Acta 71, 305–325.
Metwally, S.S., Ghaly, M., El-Sherief, E.A., 2017. Physicochemical properties of synthetic nano-birnessite and its enhanced scavenging of Co^{2+} and Sr^{2+} ions from aqueous solutions. Mater. Chem. Phys. 193, 63–72.
Missana, T., Garcia-Gutierrez, M., 2007. Adsorption of bivalent ions (Ca(II), Sr(II) and Co (II)) onto FEBEX bentonite. Phys. Chem. Earth 32, 559–567.
Missana, T., Garcia-Gutierrez, M., Alonso, U., 2008. Sorption of strontium onto illite/smectite mixed clays. Phys. Chem. Earth 33, S156–S162.
Missana, T., Alonso, U., Garcia-Gutierrez, M., 2009. Experimental study and modelling of selenite sorption onto illite and smectite clays. J. Colloid Interface Sci. 334, 132–138.
Missana, T., Benedicto, A., Mayordomo, N., Alonso, U., 2014. Analysis of anion adsorption effects on alumina nanoparticles stability. Appl. Geochem. 49, 68–76.
Mukhopadhyay, J., Sengupta, P., Sen, D., Mazumdar, S., Tyagi, A.K., 2015. Uptake of Cs and Sr radionuclides within oleic acid coated nanomagnetite-hematite composite. J. Nucl. Mater. 467, 512–518.
Nie, Z., Finck, N., Heberling, F., Pruessmann, T., Liu, C., Lützenkirchen, J., 2017. Adsorption of selenium and strontium on goethite: EXAFS study and surface complexation modeling of the ternary systems. Environ. Sci. Technol. 51, 3751–3758.
Nielsen, S.P., 2004. The biological role of strontium. Bone 35, 583–588.
Ohnuki, T., Kozai, N., 1994. Sorption characteristics of radioactive cesium and strontium on smectite. Radiochim. Acta 66/67, 327–331.
Pathak, P., 2017. An assessment of strontium sorption onto bentonite buffer material in waste repository. Environ. Sci. Pollut. Res. 24, 8825–8836.
Powell, K.J., Brown, P.L., Byrne, R.H., Gajda, T., Hefter, G., Sjöberg, S., Wanner, H., 2011. Chemical speciation of environmentally significant metals with inorganic ligands Part 4: the Cd^{2+} + OH^-, Cl^-, CO_3^{2-}, SO_4^{2-} and PO_4^{3-} systems. Int. Union Pure Appl. Chem. 83, 1163–1214.
Pusch, R., Kasbohm, J., Knutsson, S., Yang, T., Nguyen-Thanh, L., 2015. The role of smectite clay barriers for isolating high-level radioactive waste (HLW) in shallow and deep repositories. Procedia Earth Planet. Sci. 15, 680–687.
Rafferty, P., Shiao, S.Y., Binz, C.M., Meyer, R.E., 1981. Adsorption of Sr(II) on clay minerals: effects of salt concentration, loading, and pH. J. Inorg. Nucl. Chem. 43, 797–805.
Rosenberg, B.L., Ball, J.E., Shozugawa, K., Korschinek, G., Hori, M., Nanba, K., Johnson, T.E., Brandl, A., Steinhauser, G., 2017. Radionuclide pollution inside the Fukushima Daiichi exclusion zone, part 1: depth profiles of radiocesium and strontium-90 in soil. Appl. Geochem. 85, 201–208.
Ryu, J., Kim, S., Hong, H.-J., Hong, J., Kim, M., Ryu, T., Park, I.-S., Chung, K.-S., Jang, J.S., Kim, B.-G., 2016. Strontium ion (Sr^{2+}) separation from seawater by hydrothermally structured titanate nanotubes: removal *vs.* recovery. Chem. Eng. J. 304, 503–510.
Sahoo, S.K., Kavasi, N., Sorimachi, A., Arae, H., Tokonami, S., Mietelski, J.W., Lokas, E., Yoshida, S., 2016. Strontium-90 activity concentration in soil samples from the exclusion zone of the Fukushima daiichi nuclear power plant. Sci. Rep. 6, 23925.
Savoye, S., Beaucaire, C., Grenut, B., Fayette, A., 2015. Impact of the solution ionic strength on strontium diffusion through the Callovo-Oxfordian clayrocks: an experimental and modeling study. Appl. Geochem. 61, 41–52.
Sharma, Y.C., Srivastava, V., Singh, V.K., Kaul, S.N., Weng, C.H., 2009. Nano-adsorbents for the removal of metallic pollutants from water and wastewater. Environ. Technol. 30, 583–609.
Shirai, T., Watanabe, H., Fuji, M., Takahashi, M., 2009. Structural properties and surface characteristics on aluminium oxide powders. Annu. Rep. Ceram. Res. Lab. Nagoya Inst. Technol. 9, 23–31.
Sid Kalal, H., Abdollahi, M., Ashoor, M., Seyedkalal, E., 2016. D2EHPA-impregnated alumina for adsorption of strontium ions in environmental samples. Int. J. Environ. Sci. Technol. 13, 1311–1318.
Siroux, B., Beaucaire, C., Tabarant, M., Benedetti, M.F., Reiller, P.E., 2017. Adsorption of strontium and caesium onto a Na-MX80 bentonite: experiments and building of a coherent thermodynamic modelling. Appl. Geochem. 87, 167–175.
Smiciklas, I., Dimovic, S., Jovic, M., Milenkovic, A., Sljivic-Ivanovic, M., 2015a. Evaluation study of cobalt(II) and strontium(II) sorption-desorption behavior for selection of soil remediation technology. Int. J. Environ. Sci. Technol. 12, 3853–3862.
Smiciklas, I., Jovic, M., Sljivic-Ivanovic, M., Mrvic, V., Cakmak, D., Dimovic, S., 2015b. Correlation of Sr^{2+} retention and distribution with properties of different soil types. Geoderma 253–254, 21–29.
Smith, K.S., 1999. Metal Sorption on Mineral Surfaces: an Overview with Examples Related to Mineral Deposits. Reviews in Economic Geology, vols. 6A and 6B Society of Economic Geologists, Inc (Chapter 7).
Sposito, G., Skipper, N.T., Sutton, R., Park, S., Soper, K., Greathouse, J., 1999. Surface geochemistry of the clay minerals. Proc. Natl. Acad. Sci. U.S.A. 96, 3358–3364.
Szczepaniak, W., Koscielna, H., 2002. Specific adsorption of halogen anions on hydrous γ-Al2O3. Anal. Chim. Acta 470, 263–276.
Testoni, R., Levizzari, R., De Salve, M., 2017. Analysis on distribution coefficients of Strontium and Cesium for safety assessment studies. J. Radioanal. Nucl. Chem. 312, 305–316.
Thoegen, T., Hummel, W., Berner, U., Curti, E., 2014. The PSI/Nagra Chemical Thermodynamic Database 12/07 (Switzerland).
Tu, Y.J., You, C.F., Chen, Y.R., Huang, C.P., Huang, Y.H., 2015. Application of recycled iron oxide for adsorptive removal of strontium. J. Taiwan Inst. Chem. Eng. 53, 92–97.
van der Lee, J., de Wint, L., 1999. Chess Tutorial and Cookbook. Technical Repot LHM/RD/99/05. .
Voronina, A.V., Semenishchev, V.S., 2016. Mechanism of strontium sorption by the mixed nickel-potassium ferrocyanide based on hydrated titanium dioxide. J. Radiooanalytical Nucl. Chem. 307, 577–590.
WHO, 2010. Concise International Chemical Assessment Document 77: Strontium and Strontium Compounds.

Yates, D.E., Levine, S., Healy, T.W., 1973. Site-binding model of the electrical double layer at the oxide/water interface. J. Chem. Soc. Faraday Trans. 1 Phys. Chem. Condens. Phases 70, 1807–1818.
Yu, S., Mei, H., Chen, X., Tan, X., Ahmad, B., Alsaedi, A., Hayat, T., Wang, X., 2015. Impact of environmental conditions on the sorption behavior of radionuclide ^{90}Sr(II) on Na-montmorillonite. J. Mol. Liq. 203, 39–46.
Zhang, N., Liu, S.J., Jiang, L., Luo, M.B., Chi, C.X., Ma, J.G., 2015. Adsorption of strontium from aqueous solution by silica mesoporous SBA-15. J. Radionalytical Nucl. Chem. 303 (3), 1671–1677.